Effect of high spontaneous polarization on defect structures and orientational dynamics of tilted chiral smectic freely suspended films

Darren R. Link,[1,*] Nattaporn Chattham,[1] Joseph E. Maclennan,[1] and Noel A. Clark[1]
[1]*Department of Physics, and Ferroelectric Liquid Crystal Materials Research Center, University of Colorado, Boulder, Colorado 80309-0390, USA*
(Received 29 September 2004; published 10 February 2005)

The director structure around topological defects and in 2π walls in the two-dimensional orientation field of thin freely suspended films of tilted chiral smectic liquid crystal is observed to minimize splay of the spontaneous polarization. Concentric ring patterns in the director field unwind more slowly in higher polarization films. These experiments confirm that polarization space charge increases the effective elasticity of static polarization-splay distortions and that it attracts ionic charge, leading to an increase in the effective orientational viscosity of the director field.

DOI: 10.1103/PhysRevE.71.021704 PACS number(s): 61.30.Jf, 61.30.Eb, 61.30.Gd, 61.30.Dk

I. INTRODUCTION

A freely suspended film of smectic liquid crystal can be thought of as a stack of two-dimensional (2D) fluid layers where the average orientation of the long axis of the rodlike molecules $\hat{\mathbf{n}}$ is either along the layer normal $\hat{\mathbf{z}}$, as in the smectic *A* phase, or tilted from $\hat{\mathbf{z}}$ by an angle ψ, as shown in Fig. 1. In the tilted smectic phases, the projection of $\hat{\mathbf{n}}$ onto the film plane defines the 2D **c**-director field, $\hat{\mathbf{c}}(\mathbf{r})$, with azimuthal orientation $\varphi(\mathbf{r})$ [1]. In the smectic *C* (Sm-*C*) phase, the molecular tilt is synclinic, uniform from layer to layer, giving a nonpolar structure with C_{2h} symmetry. When the molecules are chiral, however, there is no mirror plane, the symmetry being only C_2, and a net (chirality-induced) spontaneous polarization is allowed perpendicular to the molecular tilt plane [2]. Hence, chiral Sm-*C* films (Sm-*C**) are ferroelectric, with a polarization (dipole moment per unit area) $\mathbf{P}(\mathbf{r})$ perpendicular to $\hat{\mathbf{c}}$. Similarly, in the case of the chiral anticlinic smectic-C_A (Sm-C_A^*) phase, where the molecular tilt direction alternates in adjacent layers, chirality results in antiferroelectric ordering of the polarization [3,4], with the result that in films with odd layer number *N*, the net spontaneous polarization is transverse (P_T, normal to both **c** and $\hat{\mathbf{z}}$), while in even *N* films the polarization is longitudinal (P_L, coplanar with **c** and $\hat{\mathbf{z}}$) [5,6]. In general, chirality also allows helixing of the director along $\hat{\mathbf{z}}$, although this effect is negligible in thin films such as those studied here.

Thin freely suspended films of achiral Sm-*C* films are well described by a 2D *XY* model, with the elastic free energy expressed in terms of the orientation of the **c**-director field of the top layer as

$$F_{elastic} = \int \left(\frac{K_S}{2} (\boldsymbol{\nabla} \cdot \hat{\mathbf{c}})^2 + \frac{K_B}{2} (\hat{\mathbf{z}} \cdot \boldsymbol{\nabla} \times \hat{\mathbf{c}})^2 \right) d^2x. \quad (1)$$

The two-dimensional splay and bend elastic constants K_S and K_B are related to the bulk Frank elastic constants by $K_S = h\mathcal{K}_{11} \sin^2 \psi$ and $K_B = h(\mathcal{K}_{22} \sin^2 \psi \cos^2 \psi + \mathcal{K}_{33} \sin^4 \psi)$, where *h* is the film thickness [1]. If we assume $K_S = K_B \equiv K$, and introduce a 2D viscous damping coefficient γ, the equation of motion for $\varphi(\mathbf{r}, t)$ can be written as

$$\frac{\partial \varphi}{\partial t} = \frac{K}{\gamma} \boldsymbol{\nabla}^2 \varphi = D \boldsymbol{\nabla}^2 \varphi, \quad (2)$$

where we have used the relation $\hat{\mathbf{c}}(r, \theta) = \hat{\mathbf{x}} \cos \varphi + \hat{\mathbf{y}} \sin \varphi$, and $D = K/\gamma$ is a rotational diffusion constant. The equilibrium director field (when $\partial\varphi/\partial t = 0$) is found by solving Laplace's equation, $\nabla^2 \varphi = 0$. In particular, this equation de-

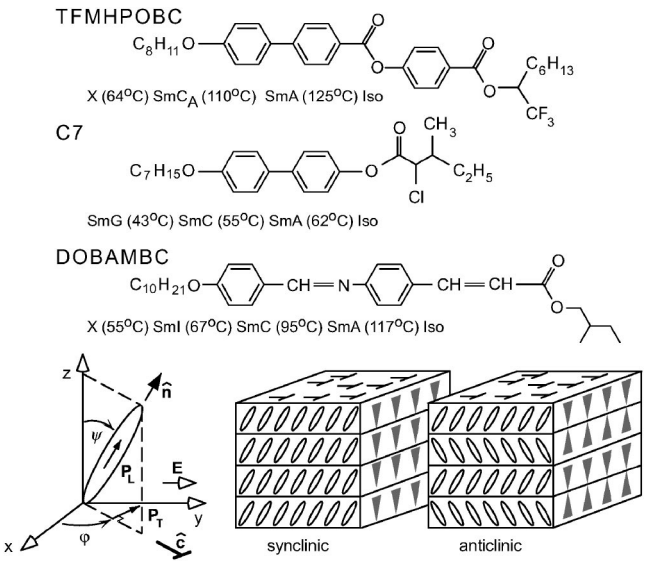

FIG. 1. Structures and phase diagrams of the liquid crystals TFMHPOBC, C7, and DOBAMBC, and molecular tilt arrangement of Sm-*C* (synclinic) and Sm-C_A (anticlinic) phases. The projection of the director $\hat{\mathbf{n}}$ onto the *x*-*y* plane defines the **c** director (⊢), which has an azimuthal orientation ϕ. In the Sm-*C* phase, the director orientation is constant from layer to layer, while in the Sm-C_A phase there is alternating tilt. P_L and P_T denote longitudinal and transverse polarizations, the latter being identically zero in nonchiral materials.

*Present address: Department of Physics, Harvard University, Cambridge, MA 02138.

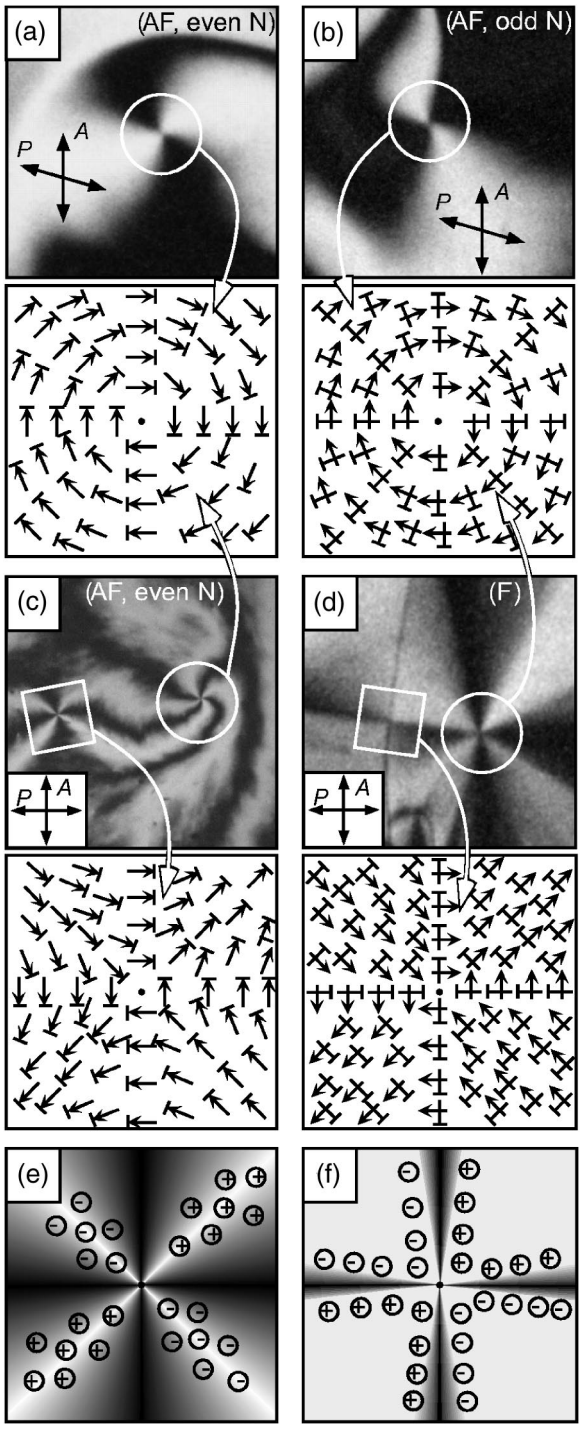

FIG. 2. DRLM images of director patterns around disclinations in tilted smectic films, along with sketches of the corresponding c-director (⊢) and polarization (→) patterns. The **c** directors are drawn for the top layer only, whereas the polarization arrows represent the in-plane component of the polarization $\mathbf{P}(\mathbf{r})$ averaged over the entire film. (a) Bend-type $s=+1$ disclination in a Sm-C_A* film of TFMHPOBC with even N. (b) Splay-type $s=+1$ disclination in a Sm-C_A* film of TFMHPOBC with odd N. (c) $s=\pm 1$ disclination pair in a Sm-C_A* film of TFMHPOBC with even N. (d) $s=\pm 1$ disclination pair in a Sm-C* film of C7. While $s=+1$ disclinations always have cylindrical symmetry [white circles in (c) and (d)], the field around $s=-1$ disclinations [white boxes in (c) and (d)] is distorted to reduce splay in the polarization [at the expense of increasing splay (bend) in $\hat{\mathbf{c}}$ when the polarization is transverse (longitudinal)]. When the polarization is very large, as in the ferroelectric C7, the charged (splayed) regions around −1 defects become very narrow, separated by large regions with uniform director orientation. (e) and (f) Polarization space charge distributions around −1 defects in films with low and high polarization, respectively (superimposed on simulated defect textures as viewed using DRLM).

scribes the static director field around disclinations or vortices, singular points in the film about which $\hat{\mathbf{c}}$ rotates through an integer number of revolutions. In cylindrical coordinates, the **c**-director field near a disclination at the origin is described by $\varphi(r,\theta)=s\theta+\alpha$, where the integer s is the strength of the disclination and α is an arbitrary angle. When freely suspended films of tilted smectics are viewed through a polarized light microscope using depolarized reflected light microscopy (DRLM), a characteristic *schlieren* texture of dark and light brushes is observed (see Figs. 2–4). The points where these dark brushes converge are the disclinations. Since the discovery of liquid crystals, such topological defects have been crucial in understanding the symmetry and phases of bulk nematics and smectics [7,8] and they are described extensively in standard texts [9,10].

In the single elastic constant model, +1 disclinations of both bend type [$\alpha=\pi/2$ or $3\pi/2$, see Fig. 2(a)] and splay type [$\alpha=0$ or π, see Fig. 2(b)] have the same free energy and would be expected to occur with equal frequency. In practice, however, the elastic constants are not equal and we find that +1 disclinations in a given film are consequently either all of bend type or all of splay type, depending on which elastic constant is smaller. Since disclinations of strength $s=-1$ [Figs. 2(c) and 2(d)] are required by their

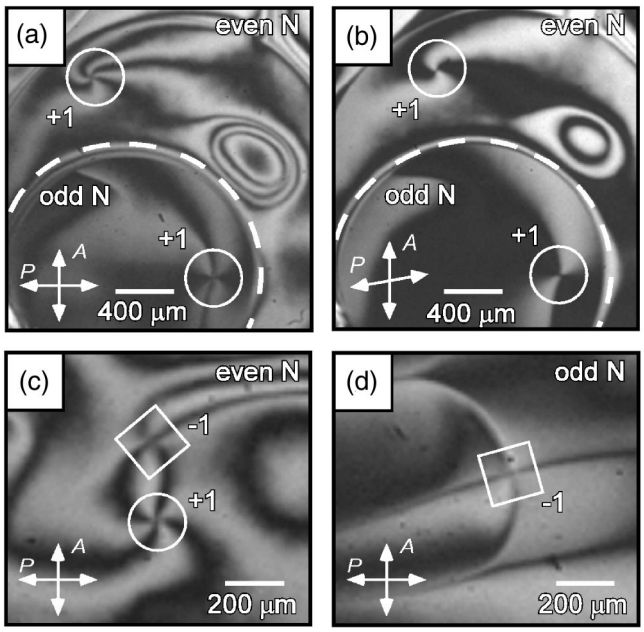

FIG. 3. Chiral TFMHPOBC film in the Sm-C_A* phase. (a) Brush patterns around +1 defects in even and odd N regions. A layer step is indicated by the dashed line. (b) By slightly decrossing the polarizer and analyzer, these defects are revealed to have different structures: in the even N region, the dark brushes are parallel to the polarizer implying that the defect is of bend type. In the odd N region, the brushes are perpendicular to the polarizer, implying **c**-director splay. (c) Pair of ±1 defects in an even N region. (d) Distorted −1 defect in an odd N region, with a director field as sketched in Fig. 2(d).

topology to be surrounded by both splay and bend distortions, anisotropy of the elastic constants results in a change in the relative widths of the bend and splay regions, with the deformation corresponding to the smaller elasticity being spatially compressed.

Purely elastic theories have been used with some success to describe, for example, the static structures of defects with anisotropic elasticity [11], disclination diffusion in two dimensions [12], defect pair annihilation [13], equilibrium structures when inclusions are present [14], and complex director structures in islands [15]. The presence of a spontaneous polarization, however, has a significant effect on the dynamic fluctuations and static structures of the director field in films [1]. In particular, splay of the polarization gives rise to space charge, $\delta(\mathbf{r}) = -\boldsymbol{\nabla} \cdot \mathbf{P}$, which makes an electrostatic contribution to the free energy [2]

$$F_{\text{dipoles}} = \frac{1}{2} \int \boldsymbol{\nabla} \cdot \mathbf{P}(\mathbf{r}) \int \frac{\boldsymbol{\nabla} \cdot \mathbf{P}(\mathbf{r}')}{|\mathbf{r} - \mathbf{r}'|} d^2x' \, d^2x. \qquad (3)$$

This may be expressed in a modal expansion of the total free energy as

$$F_q = \int \left(\frac{K_S}{2} q_{\parallel}{}^2 + \frac{K_B}{2} q_{\perp}{}^2 + 2\pi P^2 q_P \right) \phi_q{}^2 d^2x, \qquad (4)$$

where ϕ_q is the amplitude of the **c**-director fluctuation with

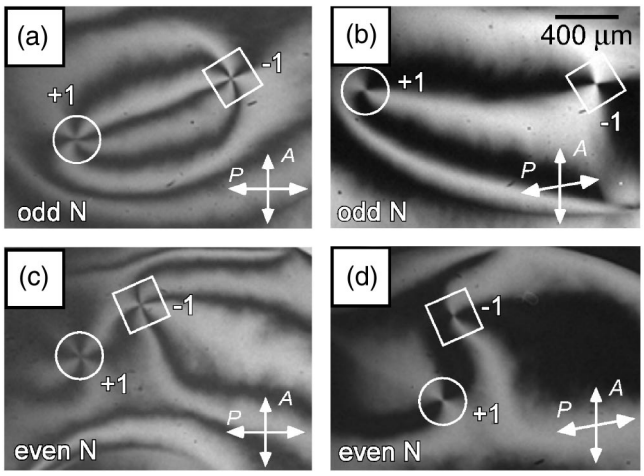

FIG. 4. Racemic TFMHPOBC film in the anticlinic Sm-C_A phase. The photomicrographs show ±1 defect pairs [(a) and (b)] in an odd N region (with no net average polarization) and [(c) and (d)] in an even N region (with longitudinal polarization). The −1 defect structure is slightly distorted in both cases, minimizing polarization splay as discussed in the text. Decrossing the polarizer and analyzer slightly [(b) and (d)] reveals that both +1 defects are of bend type. The scale in all images is the same.

wave vector $\mathbf{q}$, $q_{\parallel}$ and $q_{\perp}$ are the components of $\mathbf{q}$ parallel and perpendicular to the tilt plane, and q_P is the component along $\mathbf{P}$. This leads to an increase in the effective elasticity for certain modes, as confirmed in extensive dynamic light scattering experiments on Sm-C* films and cells, where significant quenching of bend mode director fluctuations has been observed [1,16,17]. This effect also qualitatively explains the large difference in the magnitude of director fluctuations observed in Sm-C* and Sm-C_A* films [5].

In 1979, Pelcovits and Halperin described theoretically how space charge should affect static structures in tilted chiral films, although the ferroelectric LC materials available at the time had extremely low polarization and were not particularly pure [18]. While it had been demonstrated that polarization splay results in an enhanced restoring force for thermal orientational director fluctuations in films [1], it appeared that ionic impurities in liquid crystals effectively screened out the space charge in static structures, canceling its effects [19]. Nevertheless, the effects of impurities were noted in the original free film studies at Harvard [1,16], and their influence on the slow dynamics of director fluctuations were later confirmed in bulk light scattering experiments [17]. Ions have since been observed to affect the shape of layer dislocations in films [20], and computer simulations of the dynamic response of chiral films suggest that ions change the shape and hence the velocity of π walls moving in response to applied electric fields [21].

Although the predicted effects of polarization charge on the texture of chiral films are expected to be screened to some extent in any material that contains ionic impurities, recent experiments, described in detail below, confirm that the polarization can nevertheless strongly affect the static director field in some LC systems, for example, around disclinations. We have also studied the relaxation of ring patterns in the director field of chiral Sm-C_A* films, where the

magnitude of the polarization, correlated with smectic layer number N, produces a striking odd-even effect in their appearance and in their relaxation dynamics. Finally, we show that the orientational dynamics of high polarization films are strongly influenced by the presence of ions.

II. DEFECT STRUCTURES

Films from $N=2$–10 smectic layers of chiral and racemic TFMHPOBC [22] and of chiral C7 [23], respectively, in the Sm-C_A*, Sm-C_A, and Sm-C* phases, were drawn across a 4-mm-diam hole in a microscope glass coverslip. The chemical structures and phase transitions of the materials studied are shown in Fig. 1. The film thickness was determined by laser reflectivity and the textures were studied using DRLM with slightly oblique incidence. To supplement the disclinations that appeared spontaneously, additional topological defects could be generated by dragging the glass spreader quickly but carefully sideways across the edge of a freshly made film. This disturbance would result in the appearance of a number of $s=\pm 1$ disclination pairs. These then diffused further onto the film, forming a disperse ensemble of weakly associated point defects that slowly coarsened through pair annihilation.

Although both +1 and −1 defects exhibit four-arm brushes under crossed polarizers [see Fig. 3(c)], they can be distinguished because +1 defects have C_∞ symmetry around their cores while −1 defects have only C_{2v} symmetry, with two orthogonal mirror planes bisecting the C_2 axis. This means, for example, for the defects shown in Figs. 2 and 3, where $\alpha=m\pi/2$, with m an integer, that the dark brushes of +1 defects always lie along the polarizer axes, while the dark brushes of −1 defects lie along the polarizer axes only if the mirror planes happen to be aligned with the crossed polarizers or are oriented at 45° to them.

The odd-even effect in the spontaneous polarization of Sm-C_A* films makes antiferroelectrics a natural choice for investigating the effect of polarization on defect structures. For $s=+1$ disclinations, we find in every case that the **c** director orients so as to reduce splay in the polarization. This means that for films of materials such as TFMHPOBC, which show transverse (longitudinal) polarization, respectively, in odd (even) N films, there is a corresponding odd-even effect in topological defect type: $s=+1$ disclinations have only bend in $\hat{\mathbf{c}}$ when N is even and only splay in $\hat{\mathbf{c}}$ when N is odd [see Figs. 2(a) and 2(b)]. While $s=+1$ defects [white circles in Figs. 2(c) and 2(d)] are always cylindrically symmetric (with constant $\partial\phi/\partial\theta$), we find that the director field of $s=-1$ disclinations [white boxes in Figs. 2(c) and 2(d)] is distorted to minimize splay in the polarization (at the expense of increasing bend): splayed regions become very broad, while bend regions are narrow. In high polarization materials, such as TFMHPOBC, these distortions can become extreme. Analogous observations are made with high polarization liquid crystals in the Sm-C* phase. In the material C7, for example, −1 defects are highly distorted, as illustrated dramatically in Fig. 2(d). Demikhov described the sharp brush patterns associated with arrays of point defects in C7 films as a "chessboard" texture and proposed that their structure was driven by a preference for minimizing the polarization charge [24].

Bend and splay type +1 defects may be distinguished experimentally by slightly decrossing the polarizer and analyzer, reducing the four brushes [Fig. 3(a)] to two [Fig. 3(b)]: when these brushes near the defect core are aligned parallel to the polarizer, the defect has bend structure, as seen in the even N region of Fig. 3(b); brushes oriented perpendicular to the polarizer, on the other hand, imply **c**-director splay structure around the defect, as in the odd N region of Fig. 3(b).

Figures 3(c) and 3(d) illustrate the effects of space charge on −1 defects in chiral TFMHPOBC. The brushes of a −1 defect in an even N film [Fig. 3(c)] are seen to be slightly narrower than those of the +1 defect. In an odd N film, with higher polarization [5], the brushes are much narrower [Fig. 3(d)], indicating that the director field is highly distorted here, as in Fig. 2(d).

Films of racemic TFMHPOBC in the Sm-C_A phase have also been investigated. Figure 4 shows ±1 defect pairs in odd and even N films in this phase, which have, respectively, $P=0$ and longitudinal polarization P_L [25]. In both cases, +1 defects exhibit bend structure, while the −1 defects are weakly distorted, with brushes slightly narrower than those of the +1 defects. The texture of the even N regions can be explained using the same arguments as for Sm-C_A* films, since they have the same polarization [5]. The C_{2h} symmetry of odd N films of the achiral material does not allow a net spontaneous polarization. However, while the longitudinal polarizations at the two surfaces cancel on average, any instance of director splay in the film leads to the creation of polarization charges of opposite sign at the two surfaces. The associated increase in electrostatic free energy results in higher splay elasticity [1].

III. RING PATTERN ANISOTROPY

The effects of high polarization are also manifest in ring patterns in the **c**-director field of Sm-C_A* films, where there is a striking odd-even effect in their appearance and relaxation dynamics correlated with smectic layer number N: not only is there an obvious difference in the relative widths of the splay and bend parts of the rings [27], but, as we will see in the next section, the relaxation times of the rings differ by an order of magnitude in odd an even films [26].

Ring patterns form spontaneously in tilted chiral films subjected to a rotating E field of appropriate strength and frequency (see [26] and references therein). These patterns consist either of sets of concentric, circular 2π walls or of a single spiraling 2π wall that terminates at an $s=+1$ point defect in the center of the pattern. When the field is removed, the ring pattern relaxes, the film eventually returning to a uniform *schlieren* texture [9]. In ring patterns in Sm-C_A* films, the anisotropy of the widths of bend and splay walls reverses in even and odd N films, an effect that can be explained by polarization stiffening of the corresponding orientational rigidities.

As first pointed out by Uto *et al.* [28], when the **c**-director field forms a series of concentric π walls, regions of pure

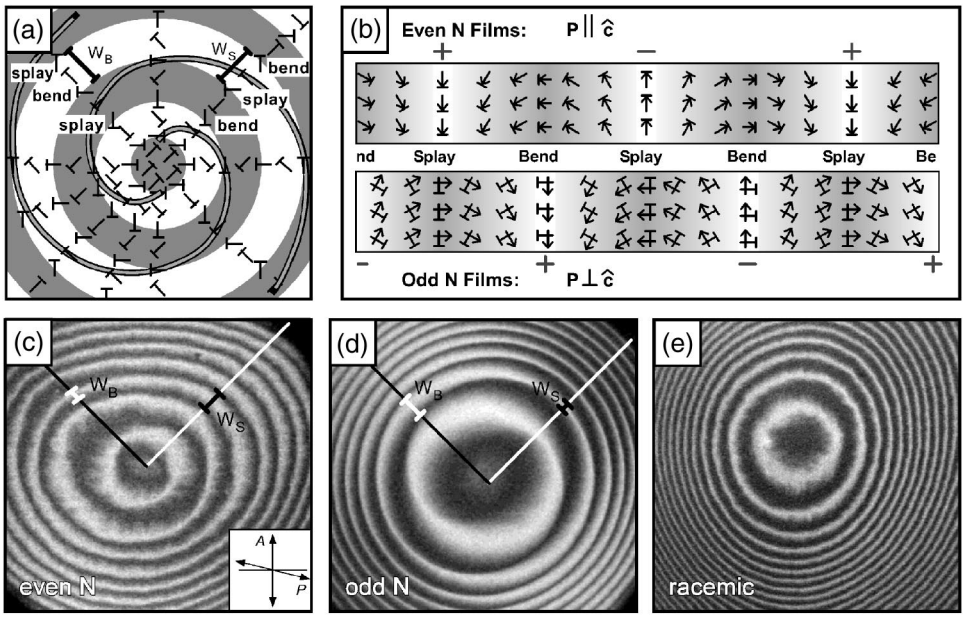

FIG. 5. Ring pattern anisotropy in antiferroelectric films. (a) As in the experiments, the rings here represent contours of constant **c**-director orientation, the character of the radial director distortion across a given ring alternating between splay and bend around its circumference. (b) A 2π rotation of the **c** director in polar films generates polarization space charge. In even N films (where $P_L \| \hat{\mathbf{c}}$), the space charge is greatest where the **c** director is splayed, while in odd N films (where $P_T \perp \hat{\mathbf{c}}$) the charge is concentrated where there is **c**-director bend. (c) and (d) Reversal of bend and splay anisotropy in Sm-C_A* TFMHPOBC films with odd and even N. The anisotropy of the elastic constants is determined by comparing the relative widths of the white rings along the two radial lines drawn at ±45°. (c) In even N films, $W_S > W_B$ implying $K_S > K_B$, while (d) in odd N films, $W_B > W_S$ implying $K_B > K_S$. (e) In (nearly) racemic odd N films, with $P \approx 0$, the wall widths are approximately equal.

bend and pure splay form a spiral pattern, shown in Fig. 5(a). The handedness of this spiral is dependent on the sign of rotation of the **c** director. From Eqs. (3) and (4), we have seen that the polarization space charge enhances the effective elasticity for the director deformation involving $\nabla \cdot \mathbf{P}$, corresponding to bend of the **c** director in odd N films and splay in even N films, as indicated in Fig. 5(b).

The anisotropy in the ring widths is evident in the ring patterns in chiral TFMHPOBC films, illustrated in Fig. 5: for an even N film (c) the splay rigidity is greater, while for an odd N film (d) the bend rigidity is greater. This conclusion is reached by comparing the width W_B of a given white ring along the radial black line, a region of pure bend, with its width W_S along the white line, where there is pure splay. The inversion in the appearance of the rings in images (c) and (d) indicates a reversal of the effective elastic anisotropy. To confirm that the spontaneous polarization does in fact play a role in producing this effect, $N=3$ layer films of racemic TFMHPOBC (doped with a tiny amount of chiral TFMHPOBC to facilitate ring winding) were studied. These films have almost no discernible anisotropy in ring width along their radius, as can be seen in Fig. 5(e). Numerical simulations of the director field evolution in films with anisotropic elasticity yield qualitatively similar textures [27,29]. The contrast between the anisotropy of chiral films and the lack of any anisotropy in the racemate is direct visual evidence that the effective elasticity is modified by the spontaneous polarization.

IV. RING RELAXATION DYNAMICS: EXPERIMENT

We studied the relaxation of concentric ring patterns in Sm-C* DOBAMBC [30] and Sm-C_A* TFMHPOBC films by analyzing the radial director profiles $\phi(r,t)$ obtained from digitized video. We assumed that the director field in ring patterns in both ferroelectric and antiferroelectric films could be described theoretically by a truncated series of harmonic functions solving Eq. (2). The decay of the ring patterns over time was analyzed to obtain the rotational diffusion constant D [26].

The functional form proposed for $\phi(r,t)$ was found to fit the experimental director profiles very well [26], although the fits to solutions of Eq. (2) for even N films (which have low polarization) were noticeably better than for odd N films. In addition, the value for D obtained in Sm-C* DOBAMBC was about a factor of 10 lower than the value previously obtained by light scattering [19].

We also observed a significant and rather puzzling difference between the relaxation rates of ring patterns in even and odd N antiferroelectric TFMHPOBC films, with odd N films relaxing much more slowly than even N films, as can be seen in Fig. 6. This effect, which seemed initially quite counterintuitive, cannot be understood in terms of the simple theory presented so far. In the case of **c**-director fluctuations, the relatively large polarization of odd N films is argued to stiffen the films, resulting in a greatly increased effective elasticity. In the light of our previous discussion, the effec-

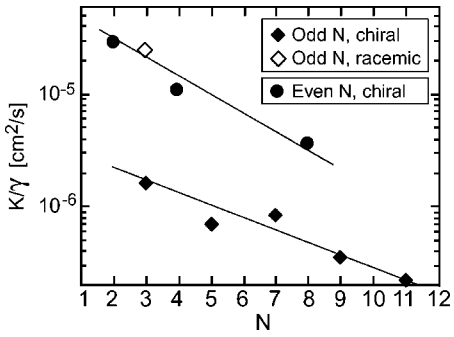

FIG. 6. Layer number dependence of the rotational diffusion constant K/γ in TFMHPOBC films in the Sm-C_A phase. All measurements were made about 5 °C below the Sm-C-Sm-C_A transition [26].

tive orientational diffusion constant D for odd N films would thus be expected to be much larger than for even N films. This would cause odd films to relax faster, whereas the opposite was in fact observed. In addition, odd N films of weakly doped racemic TFMHPOBC have large **c**-director fluctuations compared to chiral films (commensurate with their low polarization), and ring patterns in these films relax in a time comparable to (low P) $N=2$ and $N=4$ films, with D much greater than in an enantiomerically pure $N=3$ film, as can be seen in Fig. 6.

These observations suggest that while Eq. (2) does capture the essence of the director dynamics if we account for the increases in the effective elasticity manifest in Eq. (4), important additional physics related to the role of the polarization in modifying the effective viscosity is being neglected.

V. RING RELAXATION DYNAMICS: EFFECT OF ELECTRICAL CHARGE

We have seen that odd N films of enantiomerically pure TFMHPOBC (enantiomeric excess, ee=1) have much slower ring relaxation dynamics than even N films and, therefore, in terms of the simple theory, have smaller values of D. The fact that in odd N films there is a net transverse polarization P_T that is large relative to the longitudinal polarization P_L in even N films, suggests that this difference, like the defect structures discussed above, may also be a polarization space charge effect. This supposition is qualitatively confirmed by the observation that in TFMHPOBC films of reduced ee (ee$\sim$0.02), D for odd N films is essentially the same as for chiral films with even N.

In this section, we develop a model for the retardation of orientation dynamics by polarization space charge, showing that screening of polarization charge by ions can have a dramatic effect on the dynamics of **c**-director structures with nonzero splay of **P** that move on the film, the coupled motion of ions increasing the dissipation associated with local change of $\mathbf{P}(\mathbf{r})$.

A key observation motivating this approach is that in odd N, enantiomerically pure films, the space charge due to divergence of $\mathbf{P}(\mathbf{r})$ produces in-plane electric fields large

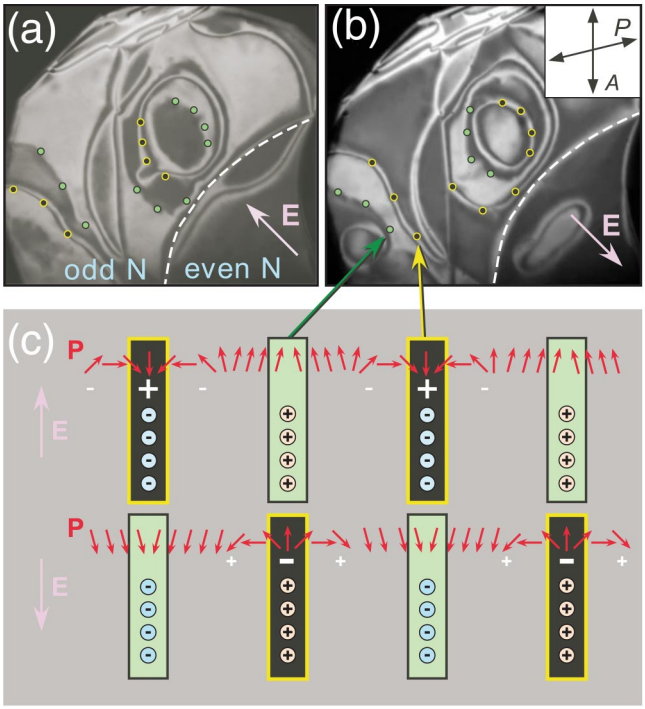

FIG. 7. (Color online) 2π walls and their "phantoms" in a Sm-C_A* TFMHPOBC film. The DRLM photomicrographs, obtained with decrossed polarizers in an applied electric field, show an area with odd and even N layer number regions. The applied field E stabilizes 2π walls in the **c**-director field [marked with open circles (green online) in (a) and (b) and with open rectangles (green online) in (c)]. Polarization splay in the walls produces polarization space charge, attracting free charges of the opposite sign. When the sign of the E field changes, the 2π walls split into pairs of π walls. These move away from each other, eventually joining with neighboring π walls to form new 2π walls centered between the original set, as sketched in (c). Free charge attracted to the original 2π walls is not redistributed instantaneously upon field reversal, resulting in "phantom" walls. These ghost images of the former 2π walls [marked with dots in (a) and (b) and with bars in (c)] disappear slowly, well after the main **c**-director reorientation has been completed. This effect is clearly evident in the odd N region, which has high polarization, while in the even N area it is not visible.

enough to segregate the ionic impurities on the films which, in turn, produce electric fields significant enough to be observable in the **c**-director patterns. Thus, as is shown in Fig. 7, stabilizing a 2π wall with an applied field and then sweeping it away by reversing the field leaves a transient "shadow" in an otherwise almost uniform **c**-director field, this ghost image being produced by ions attracted by the polarization charge density δ and partially screening it. Once the polarization field is rendered nearly uniform by electric field reversal, the ions drift away and the shadow disappears over a period of a few minutes.

Analysis of such effects begins with consideration of the dynamics of the relaxation of surface charge density due to ions in the film plane, $\rho(\mathbf{r},t)$, which we obtain via Fourier transformation of the time-dependent amplitudes $\rho_q(t)$ of ion charge density waves (CDWs) of wave vector $\mathbf{q}$. For a three-dimensional medium of bulk electrical conductivity σ_B and

dielectric constant ε, an initial volume charge density decays exponentially in time toward electrostatic equilibrium, with a relaxation time [31]

$$\tau_B = \frac{\varepsilon}{\sigma_B}$$

which does not depend on wave vector. To obtain the equivalent expression for a thin film (i.e., with $qh \ll 1$), we use a static CDW $\rho(\mathbf{r},t) = \rho q \exp iqx$ with wavefronts parallel to the y axis. The areal charge density is $\rho(\mathbf{r},t)h$ and the electric field produced by this charge $[\boldsymbol{\nabla}\cdot\mathbf{E}(\mathbf{r},t) = \rho(\mathbf{r},t)/\varepsilon_0]$ is

$$\mathbf{E}(x,y) = \frac{\rho q h}{2\varepsilon_0}\{\mathbf{y}\ \exp(iqx - q|y|) + \mathbf{x}(-i)\exp(iqx - q|y|)\}.$$

From charge continuity,

$$\frac{\partial \rho}{\partial t} = -\ \boldsymbol{\nabla}\ \cdot \mathbf{J} = -\frac{\partial}{\partial_x}(\sigma_B E_x),$$

yielding

$$(2\varepsilon_0/h)\ \partial E_x/\partial t = -\ q\sigma_B E_x.$$

Defining $\sigma_F = \sigma_B h$ and $\tau_F(q)$ by $\partial E_x/\partial t = -E_x/\tau_F(q)$, we find

$$\tau_F(q) = \frac{2\varepsilon_0}{q\sigma_F}.$$

In summary, charge density waves in thin films also decay exponentially, but with a wave-vector-dependent relaxation time.

The dielectric constant of the medium surrounding the film (air in this case) is taken here to be equal to ε_0, the permittivity of free space, σ_B is the effective bulk conductivity of the liquid crystal, and $\sigma_F = \sigma_B h$ is the effective 2D sheet conductivity of the film. Note that in the film, the q^{-1} dependence makes the relaxation relatively slower at longer length scales.

Next we consider the effect of this relaxation to electrostatic equilibrium on the motion of charge in the film plane, assuming that we have a polarization CDW $\delta(\mathbf{r},t) = \delta_q \exp i(qx - \omega t)$ parallel to the y axis traveling in the x direction. The resulting electric field induces an ionic charge density wave $\rho(\mathbf{r},t) = \rho_q \exp i(qx - \omega t)$ of steady-state amplitude ρ_q, which we find to be

$$\rho_q = \frac{-\delta_q}{1 - i\omega\tau_F(q)} = \frac{-\delta_q}{1 - ic(2\varepsilon_o/\sigma_B h)} = \frac{-\delta_q}{1 - i(c/c_F)}.$$

Here $c = \omega/q$ is the traveling velocity of the polarization CDW and $c_F = \sigma_F/2\varepsilon_o$ has dimensions of velocity. In the limit of slow motion ($c \ll c_F$), we have $\rho_q = -\delta_q$ and the polarization charge will be completely screened by ions. However, the screening becomes less complete as c increases. For c/c_F small but nonzero, the incomplete screening puts the ion CDW slightly out of phase with the polarization CDW, generating an electric field $E(\mathbf{r})$ of amplitude $E_q = +(\rho_q/2\varepsilon_o)(c/c_F)$. This in turn acts on the polarization charge to produce an average drag force/area $\langle \mathcal{F}(\mathbf{r})\rangle = \langle \delta(\mathbf{r})E(\mathbf{r})\rangle = \Re(\delta_q E_q{}^*/2)$. The inverse mobility of the CDW is then

$$\mu(c)^{-1} = \frac{\langle \mathcal{F}\rangle}{c} = \frac{\delta_q{}^2/2\sigma_F}{1 + (c/c_F)^2}. \tag{5}$$

The drag thus increases strongly with polarization charge density and exhibits behavior akin to shear-thinning, decreasing with increasing velocity for $c > c_F$.

This result is readily generalized to a localized reorientation of the **c** director with an associated polarization charge density. Consider, for example, a 2π wall stabilized by an in-plane electric field and subject to a rapid field reversal: the 2π wall splits into two π walls, which move from the center of the 2π wall, leaving behind the orientation of the **c** director now preferred by the (reversed) field. Each π wall necessarily generates polarization splay and will have a localized charge density "pulse" $\delta(x,t) = \delta_0 g(x - ct)$, where g is a dimensionless function, oriented parallel to the y axis and moving in the x direction. The above calculation for $\mu(c)^{-1}$ for a sinusoidal CDW is readily generalized using Fourier superposition to the case of an arbitrary charge density localized to a linear wall. The inverse mobility of such a wall in the presence of ions is given by

$$M_i^{-1}(c) = \frac{f}{c} = \frac{(1/2\sigma_F)\delta_0{}^2 \int g(x)^2 dx}{1 + (c/c_F)^2},$$

which exhibits the same general features as the simple sinusoidal case. Here f is the drag force per unit length on the wall.

The key parameters controlling these charge relaxation effects, $\tau_F(q)$ and c_F, can be estimated simply from qualitative observation of the relaxation of the shadow effect illustrated in Fig. 7. Typically we find $\tau_F(q) = 2\tau_B/qh \sim 20$ s for $q \sim 100\ \mathrm{cm}^{-1}$ and $h \sim 100$ Å. This value of $\tau_F(q)$ would correspond to a bulk liquid crystal relaxation time $\tau_B = qh\tau_F(q)/2$ of $\tau_B \sim 1$ ms, a value consistent with ion concentrations $\rho \sim 10^{12}$ ions/cm^3, a reasonable value for the samples used, which were not specifically deionized. In this case, $c_F = 1/q\tau_F \sim 10\ \mu$m/s. In the ring relaxation experiments, the largest CDW velocity is $c \sim 10\ \mu$m/s right at the center of the ring pattern and is smaller everywhere else, putting the experiments in the low-c ($c < c_F$) regime of Eq. (5).

Next we compare the magnitude of the ion-induced drag on a moving reorientation wall relative to that due to orientational viscosity. For a wall of width ξ moving with velocity c, the viscous energy dissipated per unit length is $u_\gamma \sim \gamma(c/\xi)^2\xi$, yielding a damping force per unit length $f_\gamma \sim \gamma c/\xi$, and a viscous inverse mobility $M_\gamma^{-1} \sim \gamma/\xi$. In the low-$c$ regime, the ion inverse mobility is $M_i^{-1} = (1/2\sigma_F)\int \delta(x)^2 dx$. For a moving wall of width ξ in a film of polarization **P**, we have $\delta \sim P/\xi$, so that $\int \delta(x)^2 dx \sim P^2/\xi$ and $M_i^{-1} \sim P^2/2\sigma_F$. M_γ can be related to M_i by noting that the usual electro-optic switching time in an applied field E is given by $\tau \sim \gamma/PE$. For a field of magnitude $E_P = P/h\varepsilon$, the internal polarization screening field, this gives $\tau_P \sim \gamma h\varepsilon/P^2$, so that $P^2 \sim \gamma h\varepsilon/\tau_P$ and $M_i^{-1} \sim \gamma h\varepsilon/\tau_P \xi\sigma_F$. With this result, we obtain

$$\frac{M_\gamma}{M_i} \sim \frac{h\varepsilon}{\tau_P \sigma_F} = \frac{\varepsilon}{\tau_P \sigma_B} = \frac{\tau_B}{\tau_P},$$

or

$$\frac{M_\gamma}{M_i} \sim \frac{\tau_B}{\tau_P}.$$

For large P materials such as TFMHPOBC, τ_P is typically 10–100 μs, which, with $\tau_B \sim 1$ ms, makes $10 < M_\gamma/M_i < 100$, easily in the range to give the polarization-induced mobility reduction manifest in the slowing down of ring relaxation in odd N films of TFMHPOBC relative to the even N and low ee films. Numerical simulations by Stannarius and Langer, based on a somewhat different theoretical approach, predict that π wall velocities may be reduced by a factor of as much as 3 or 4 in the presence of typical ion concentrations [21].

VI. SUMMARY

When there is a net spontaneous polarization in tilted fluid smectic films, polarization charge arising from spatial variations of the molecular orientation effectively increases the orientational rigidity of the director field, acting to minimize and spatially confine polarization splay. These effects can be observed directly around topological defects and in the spatial anisotropy of ring patterns in the director field. The reorientation dynamics of 2π walls is also strongly influenced by the magnitude of the spontaneous polarization, there being, for example, a dramatic alternation between fast and slow relaxation in even and odd N films. We have shown that ionic impurities, attracted to regions with high polarization space charge, increase the effective orientational viscosity of the film, leading to a retardation in the orientational dynamics of the director field.

ACKNOWLEDGMENTS

We wish to thank L. Radzihovsky and R. B. Meyer for fruitful discussions. This work was supported by NSF Grant No. DMR-0072989 and by NASA Grant No. NAG3-2457.

[1] C. Y. Young, R. Pindak, N. A. Clark, and R. B. Meyer, Phys. Rev. Lett. **40**, 773 (1978); C. Rosenblatt, R. Pindak, N. A. Clark, and R. B. Meyer, *ibid.* **42**, 1220 (1979).

[2] R. B. Meyer, L. Liébert, L. Strzelecki, and P. Keller, J. Phys. (Paris), Lett. **36**, L69 (1975).

[3] A. D. L. Chandani, Y. Ouchi, H. Takezoe, A. Fukuda, K. Terashima, K. Furukawa, and A. Kishi, Jpn. J. Appl. Phys., Part 2 **28**, L1261 (1989).

[4] We use the terms "ferroelectric" and "antiferroelectric" to refer to smectic phases with parallel and antiparallel arrangements of the polarization in adjacent layers—phases which do show classical ferroelectric and antiferroelectric behavior in surface-stabilized cells. See, for example, S. T. Lagerwall, *Ferroelectric and Antiferroelectric Liquid Crystals* (Wiley, New York, 1999).

[5] D. R. Link, J. E. Maclennan, and N. A. Clark, Phys. Rev. Lett. **77**, 2237 (1996).

[6] In a given material, the transverse or longitudinal polarization in the Sm-C_A* phase ($\sim P_1/N$) is generally smaller than the transverse polarization (P_1, the polarization of a single layer) in the Sm-C* phase.

[7] G. Friedel, Ann. Phys. (Paris) **18**, 273 (1922).

[8] D. Demus and L. Richter, *Textures of Liquid Crystals* (Verlag Chemie, New York, 1978).

[9] P. G. de Gennes and J. Prost, *The Physics of Liquid Crystals* (Clarendon, Oxford, 1993).

[10] S. Chandrasekhar, *Liquid Crystals* (Cambridge University Press, Cambridge, U.K.,1992).

[11] S. A. Langer and J. P. Sethna, Phys. Rev. A **34**, 5035 (1986).

[12] C. D. Muzny and N. A. Clark, Phys. Rev. Lett. **68**, 804 (1992).

[13] W. G. Jang, V. V. Ginzburg, C. D. Muzny, and N. A. Clark, Phys. Rev. E **51**, 411 (1995); V. V. Ginzburg, P. D. Beale, and N. A. Clark, *ibid.* **52**, 2583 (1995).

[14] D. Pettey, T. C. Lubensky, and D. R. Link, Liq. Cryst. **25**, 579 (1998).

[15] K.-K. Loh, I. Kraus, and R. B. Meyer, Phys. Rev. E **62**, 5115 (2000).

[16] C. Rosenblatt, R. B. Meyer, R. Pindak, and N. A. Clark, Phys. Rev. A **21**, 140 (1980).

[17] M.-H. Lu, K. A. Crandall, and C. Rosenblatt, Phys. Rev. Lett. **68**, 3575 (1992).

[18] R. A. Pelcovits and B. I. Halperin, Phys. Rev. B **19**, 4614 (1979).

[19] R. Pindak, C. Y. Young, R. B. Meyer, and N. A. Clark, Phys. Rev. Lett. **45**, 1193 (1980).

[20] R. Holyst, A. Poniewierski, P. Fortmeier, and H. Stegemeyer, Phys. Rev. Lett. **81**, 5848 (1998).

[21] R. Stannarius and C. Langer, Mol. Cryst. Liq. Cryst. Sci. Technol., Sect. A **358**, 109 (2001).

[22] TFMHPOBC is 4-(1-trifluoromethylhexyloxycarbonyl) phenyl 4′-octyloxybiphenyl-4-carboxylate [see Y. Suzuki, T. Hagiwara, I. Kawamura, N. Okamura, T. Kitazume, M. Kakimoto, Y. Imai, Y. Ouchi, H. Takezoe, and A. Fukuda, Liq. Cryst. **6**, 167 (1989); a corrected phase diagram may be found in T. Isozaki, H. Takezoe, A. Fukuda, Y. Suzuki, and I. Kawamura, J. Mater. Chem. **4**, 237 (1994)].

[23] C7 is 4-(3-methyl-2-chloropentanoyloxy)-4′- heptyloxybiphenyl [see Ch. Bahr and G. Heppke, Mol. Cryst. Liq. Cryst., Lett. Sect. **4**, 31 (1986)].

[24] E. Demikhov, Europhys. Lett. **25**, 259 (1994); E. Demikhov and H. Stegemeyer, Liq. Cryst. **18**, 37 (1995). These authors realized that the sharp boundaries observed in the "chessboard" texture implied a director field with apparent fourfold symmetry around the defects, and associated this with strength +1 defects. However, +1 defects can avoid polarization splay completely by enforcing uniform splay of the **c** director (and bend of **P**), which might be preferred over the C_4 symmetric director field with energetically costly jumps in director orientation proposed in these papers.

[25] D. R. Link, G. Natale, N. A. Clark, J. E. Maclennan, M. Walsh, S. S. Keast, and M. E. Neubert, Phys. Rev. Lett. **82**, 2508 (1999).

[26] D. R. Link, L. Radzihovsky, G. Natale, J. E. Maclennan, N. A. Clark, M. Walsh, S. S. Keast, and M. E. Neubert, Phys. Rev. Lett. **84**, 5772 (2000).

[27] D. Bundy, D. R. Link, N. A. Clark, and J. E. Maclennan (Poster presented at the 18th Int. Liq. Cryst. Conf., Sendai, 2000).

[28] S. Uto, E. Tazoh, M. Ozaki, and K. Yoshino, Jpn. J. Appl. Phys., Part 2 **36**, L1198 (1997).

[29] C. Chevallard, T. Frisch, and J. J. Gilli, J. Phys. II **7**, 1261 (1997).

[30] DOBAMBC is [(*p*-decyloxybenzylidene) *p′*-amino-2-methylbutylcinnamate] (see Ref. [2]).

[31] J. R. Reitz, F. J. Milford, and R. W. Christy, *Foundations of Electromagnetic Theory* (Addison-Wesley, Reading, MA, 1979).